Available online at www.sciencedirect.com
SCIENCE DIRECT®
Engineering Geology 70 (2003) 235–248
ENGINEERING GEOLOGY
www.elsevier.com/locate/enggeo

Flow and transport through clay membrane barriers

Michael A. Malusis[a], Charles D. Shackelford[b,*], Harold W. Olsen[c]

[a] GeoTrans, 9101 Harlan St. Suite 210, Westminster, CO 80031-2926, USA
[b] Department of Civil Engineering, Colorado State University, Fort Collins, CO 80523-1372, USA
[c] Division of Engineering, Colorado School of Mines, Golden, CO 80401, USA

Abstract

Flux equations for liquid and solute migration through clay barriers that behave as semi-permeable membranes used in waste containment and remediation applications, known as clay membrane barriers (CMBs), are discussed. The results of a simplified analysis of flow through a geosynthetic clay liner (GCL) using measured values for the chemico-osmotic efficiency coefficient (ω) of the GCL indicate a total liquid flux that counters the outward Darcy (hydraulic) flux due to chemico-osmosis associated with clay membrane behavior of the GCL. Also, the solute (contaminant) flux through the GCL is reduced relative to the solute flux that would occur in the absence of membrane behavior due to chemico-osmotic counter advection and solute restriction. Since diffusion commonly controls solute transport through GCLs and other low-permeability clay barriers, the implicit (empirical) correlation between ω and the effective salt-diffusion coefficient of the migrating contaminant is an important consideration with respect to contaminant restriction in CMBs.

Keywords: Advection; Bentonite; Chemico-osmosis; Clay barriers; Containment; Contaminant transport; Diffusion; Geosynthetic clay liner; Hyperfiltration; Membrane; Osmosis; Waste disposal

1. Introduction

1.1. Clay membrane behavior

The ability of clay soils to act as membranes that restrict the passage of solutes (e.g., aqueous miscible contaminants) is well documented (e.g., Kemper and Rollins, 1966; Olsen, 1969; Olsen et al., 1990). Restricted movement of inorganic solutes, specifically anions and cations, through the pores of a clay soil has been attributed to electrostatic repulsion of the ions by electric fields associated with the diffuse double layers (DDLs) of adjacent clay particles (e.g., Hanshaw and Coplen, 1973; Fritz, 1986; Keijzer et al., 1997). Non-electrolyte solutes (uncharged species), such as aqueous miscible organic compounds, also may be restricted from migrating through clay soils due to *steric hindrance*, i.e., the geometric restriction that results when the solute molecule is greater than the pore size (Grathwohl, 1998). The existence of membrane behavior also results in chemico-osmosis, or the movement of liquid in response to a solute concentration gradient, from lower solute concentration (higher water activity) to higher solute concentration (lower water activity) (e.g., Katchalsky and Curran, 1965; Greenberg et al., 1973; Fritz, 1986).

* Corresponding author. Tel.: +1-970-491-5051; fax: +1-970-491-3584.
E-mail address: shackel@engr.colostate.edu (C.D. Shackelford).

0013-7952/03/$ - see front matter © 2003 Elsevier B.V. All rights reserved.
doi:10.1016/S0013-7952(03)00092-9

The term "semi-permeable" pertains to any material that behaves as a membrane. The extent to which clay soils act as semi-permeable membranes traditionally has been quantified in terms of a reflection or osmotic efficiency coefficient, σ (Staverman, 1952; Katchalsky and Curran, 1965; Kemper and Rollins, 1966; Olsen et al., 1990). In cases where σ represents stress, the osmotic efficiency coefficient has been designated by ω (e.g., Mitchell, 1993). Also, in some cases, ω has been referred to as the chemico-osmotic efficiency coefficient to distinguish the osmotic flow process in response to a concentration gradient from osmotic flow processes in response to electrical gradients (i.e., electro-osmosis) or thermal gradients (i.e., thermo-osmosis) (Malusis et al., 2001; Malusis and Shackelford, 2002a). This latter terminology will be used throughout the remainder of the current presentation.

In general, ω ranges from zero representing a material that exhibits no solute restriction, to unity representing an "ideal" or "perfect" membrane that completely restricts the movement of solutes (i.e., $0 \leq \omega \leq 1$). In most cases involving membrane behavior in clay soils, only a portion of the pores is restrictive such that $0 < \omega < 1$, and the clay soils are referred to as "nonideal" or "leaky" membranes (Kemper and Rollins, 1966; Olsen, 1969; Barbour and Fredlund, 1989; Mitchell, 1993; Keijzer et al., 1997). Both "nonideal" and "ideal" membranes are semi-permeable.

1.2. Factors affecting clay membrane behavior

The value of ω is affected by several factors, including the state of stress in the soil, the types and amounts of clay minerals comprising the soil, and the types (species) and concentrations of the solutes in the pore water (Kemper and Rollins, 1966; Olsen et al., 1990; Mitchell, 1993; Malusis et al., 2001; Malusis and Shackelford, 2002a). In general, ω increases with increase in the effective stress in the soil (or decrease in void ratio or porosity), increase in the activity of the clay soil, and decrease in the solute charge and/or solute concentration (Kemper and Rollins, 1966; Olsen, 1969; Mitchell, 1993).

In particular, membrane behavior in the presence of common electrolytes (e.g., NaCl) has been illustrated extensively for sodium bentonite (e.g., Kemper and Rollins, 1966; Keijzer et al., 1997; Malusis et al., 2001; Malusis and Shackelford, 2002a). These results suggest that membrane behavior is significant in clay soils containing an appreciable amount of sodium montmorillonite. Clay soils containing sodium montmorillonite, such as sodium bentonite, also are desirable for use in waste containment barriers (e.g., soil–bentonite cutoff walls, compacted sand–bentonite liners, geosynthetic clay liners) due to the low hydraulic conductivity (e.g., $\leq 10^{-9}$ m/s) typically required in these applications (e.g., D'Appolonia, 1980; Lundgren, 1981; Gipson, 1985; Garlanger et al., 1987; Ryan, 1987; Chapuis et al., 1992; Day, 1994; O'Sadnick et al., 1995; Gleason et al., 1997; Stern and Shackelford, 1998; Jo et al., 2001; Abichou et al., 2002). Thus, the existence of membrane behavior resulting from the sodium montmorillonite content in clay soil barriers may have an effect on the migration of contaminants through such barriers.

For example, ω values for two different types of bentonite specimens are shown in Fig. 1. The data in

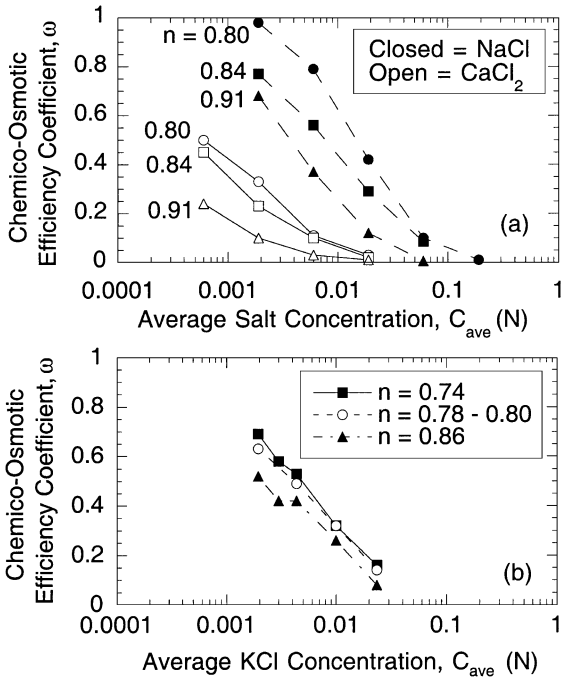

Fig. 1. Chemico-osmotic efficiency coefficients as a function of average salt concentration across the specimen and the specimen porosity (n) for (a) bentonite specimens (data from Kemper and Rollins, 1966), and (b) a geosynthetic clay liner (data from Malusis and Shackelford, 2002a).

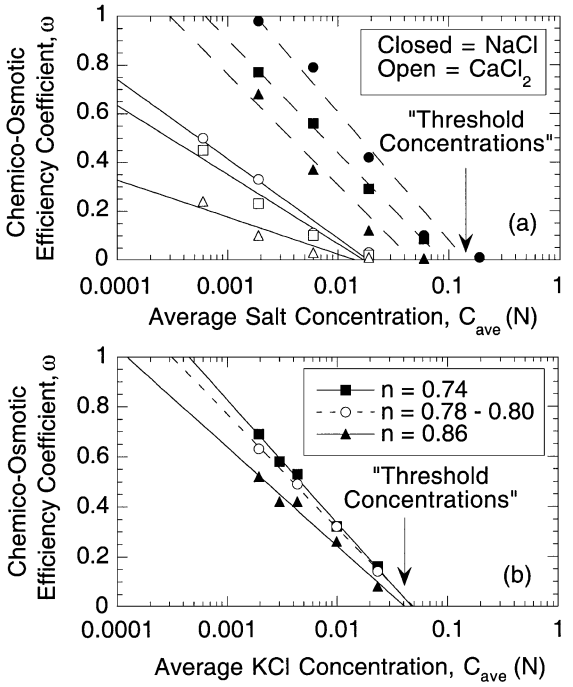

Fig. 2. Semi-log linear regressions of measured chemico-osmotic efficiency coefficients versus average salt concentration for (a) bentonite specimens (data from Kemper and Rollins, 1966), and (b) a geosynthetic clay liner (data from Malusis and Shackelford, 2002a) (n = specimen porosity).

Fig. 1 indicate that ω decreases as the salt concentration increases for a given porosity (n) and salt (NaCl or $CaCl_2$) solution, whereas the data in Fig. 1a also indicate that ω decreases with an increase in cation charge (Ca^{2+} versus Na^{+}) for a given porosity and average salt concentration. Both of these trends are consistent with expected behavior based on DDL theory in that the thickness of the DDLs of adjacent clay particles and the resulting extent of influence of the ion-restricting electric fields inside the soil pores decreases as the ion concentration and cation charge in the pore water increases (e.g., Fritz, 1986).

1.3. Limits of clay membrane behavior

Semi-log linear fits to the measured data in Fig. 1 are shown in Fig. 2. The resulting regression coefficients for the fitted functions as well as the corresponding coefficients of determination (r^2) are summarized in Table 1. As indicated by the r^2 values reported in Table 1, the majority of these fitted functions describe the measured data reasonably well. Thus, such functional fits may be useful for evaluating the limits of membrane behavior for a given solute species and clay soil exhibiting membrane behavior, such as the average "threshold" concentration at which a clay soil begins to exhibit membrane behavior (see Fig. 2).

For example, estimates of the expected limiting average salt concentrations corresponding to establishment of a semi-permeable membrane ($\omega = 0$) or to ideal membrane behavior ($\omega = 1$) based on extrapolation of the fitted functions shown in Fig. 2 are summarized in Table 1. As indicated in Table 1, semi-permeable membrane behavior for the bentonite specimens is expected to be established (i.e., $\omega = 0$) at average concentrations ranging from ~ 0.05 to ~ 0.14 N (~ 0.05 to ~ 0.14 M) for the mono-

Table 1
Results of regression analyses shown in Fig. 2

Salt	Porosity, n	Regression coefficients for: $\omega = A + B \log (C_{ave})$[a]			Limiting average concentrations, C_{ave} (N)	
		A	B	r^2	at $\omega = 0$	at $\omega = 1$
NaCl	0.80	− 0.445	− 0.526	0.970	0.142	1.79×10^{-3}
	0.84	− 0.491	− 0.465	0.997	0.0881	6.24×10^{-4}
	0.91	− 0.604	− 0.455	0.964	0.0472	3.00×10^{-4}
KCl	0.74	− 0.649	− 0.492	0.996	0.0480	4.47×10^{-4}
	0.79[b]	− 0.595	− 0.455	0.998	0.0493	3.13×10^{-4}
	0.86	− 0.547	− 0.395	0.978	0.0413	1.22×10^{-4}
$CaCl_2$	0.80	− 0.563	− 0.326	0.972	0.0187	1.60×10^{-5}
	0.84	− 0.502	− 0.284	0.953	0.0171	5.14×10^{-6}
	0.91	− 0.281	− 0.152	0.889	0.0142	3.74×10^{-9}

[a] ω = Chemico-osmotic efficiency coefficient; C_{ave} is in normality (N); r^2 = coefficient of determination.
[b] Average of range: $0.78 \le n \le 0.80$.

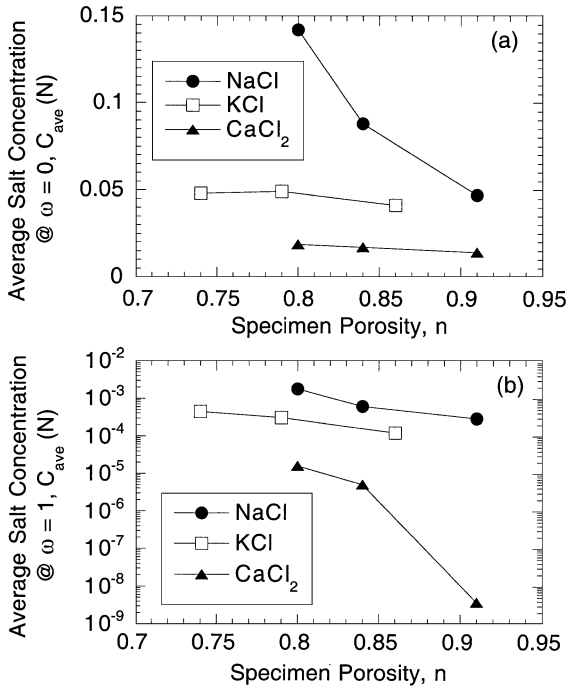

Fig. 3. Effect of specimen porosity on average salt concentrations required to establish (a) semi-permeable and (b) ideal membrane behavior for bentonite specimens identified in Fig. 1.

valent salt (NaCl or KCl) solutions, and from ~ 0.01 to ~ 0.02 N (~ 0.005 to ~ 0.01 M) for the divalent salt ($CaCl_2$) solutions. Also, ideal membrane behavior ($\omega = 1$) is expected to occur at average concentrations ranging from ~ 1×10^{-4} to ~ 2×10^{-3} N (~ 1×10^{-4} to ~ 2×10^{-3} M) for the monovalent salt (NaCl or KCl) solutions, and from ~ 4×10^{-9} to ~ 2×10^{-5} N (~ 2×10^{-9} to ~ 1×10^{-5} M) for the divalent salt ($CaCl_2$) solutions.

The effect of the specimen porosity on the limiting average concentrations corresponding to $\omega = 0$ is shown in Fig. 3. As shown in Fig. 3a, the average threshold concentration corresponding to initiation of membrane behavior for the sodium bentonite specimens is sensitive to the specimen porosity in the case of NaCl, with the average threshold concentration increasing with decreasing specimen porosity. However, in the case of the KCl and $CaCl_2$ salt solutions, specimen porosity plays a relatively minor role in terms of affecting the average threshold concentration for the range of specimen porosities shown. Thus, the effect of specimen porosity on the average threshold concentration apparently is significant only when the salt cation is the same as the dominant exchangeable cation that, in this case, is sodium (Na^+).

In the case of ideal membrane behavior (Fig. 3b), the limiting average concentration at which $\omega = 1$ tends to decrease with an increase in specimen porosity regardless of the type of salt solution. However, the effect of specimen porosity appears to be significant only in the case of the $CaCl_2$ solutions, presumably due to the greater influence of the divalent calcium cation (Ca^{2+}) on the thickness of the DDLs at all specimen porosities relative to the monovalent sodium and potassium cations (Na^+ and K^+).

1.4. Relevance of clay membrane behavior

The results summarized in Table 1 indicate that initiation of membrane behavior in the sodium bentonite specimens occurs at average threshold concentrations that are substantially lower in the case of the divalent salt solutions relative to the monovalent salt solutions, as expected on the basis of diffuse double layer (DDL) theory. This observation has important practical ramifications since most metals of environmental concern are divalent in free ionic form (e.g., Cd^{2+}, Cu^{2+}, Hg^{2+}, Ni^{2+}, Pb^{2+}, Se^{2+}, Zn^{2+}, etc.). In addition, the waste streams in many, if not most, practical applications are comprised of mixtures of

Table 2
Maximum contaminant levels (MCLs) for selected contaminants in the United States

MCL (mg/l)	Element or compound	Symbol or formula	Atomic or formula weight (g/mol)	MCL (molarity, M)
0.002	Mercury	Hg	200.59	9.97×10^{-9}
	Vinyl Chloride (VC)	C_2ClH_3	62.50	3.20×10^{-8}
0.005	Carbon Tetrachloride (CT)	CCl_4	153.84	3.25×10^{-8}
	Trichloroethylene (TCE)	C_2Cl_3H	131.38	3.81×10^{-8}
	Cadmium	Cd	112.41	4.45×10^{-8}
	Benzene (B)	C_6H_6	78.12	6.40×10^{-8}
0.05	Lead	Pb	207.2	2.41×10^{-7}
	Selenium	Se	78.96	6.33×10^{-7}
	Arsenic	As	74.92	6.67×10^{-7}
0.1	Nickel	Ni	58.70	1.70×10^{-6}

chemical species resulting in solution ionic strengths that may far exceed the threshold concentrations based on such simple divalent salt ($CaCl_2$) solutions. Thus, on the basis of these considerations, membrane behavior may not be relevant for many practical applications. However, consideration also must be given to the particular application.

For example, at some sites, traditional in situ remediation methods (e.g., pump and treat), as well as emerging in situ treatment technologies (e.g., surfactant flushing), have failed to achieve risk-based endpoints (Shackelford and Jefferis, 2000). In the case of pump and treat, the technology typically has been successful at removing a significant amount of the contaminant mass from the subsurface (e.g., >90% contaminant mass removal), but the residual concentration typically is still substantially greater than the regulated maximum concentration. As shown in Table 2, many of these regulated maximum concentrations, referred to as maximum contaminant levels or MCLs in the US, are substantially lower than the threshold concentrations shown in Table 1 required for the establishment of membrane behavior. As a result, the residual concentration in the subsurface after pump and treat may be substantially lower than the threshold concentration, but still greater than regulated maximum concentration. Thus, even though membrane behavior is primarily associated with dilute concentrations, such dilute concentrations still may exceed significantly regulated limits, such that the range of concentrations for which clay membrane behavior typically is significant also may be

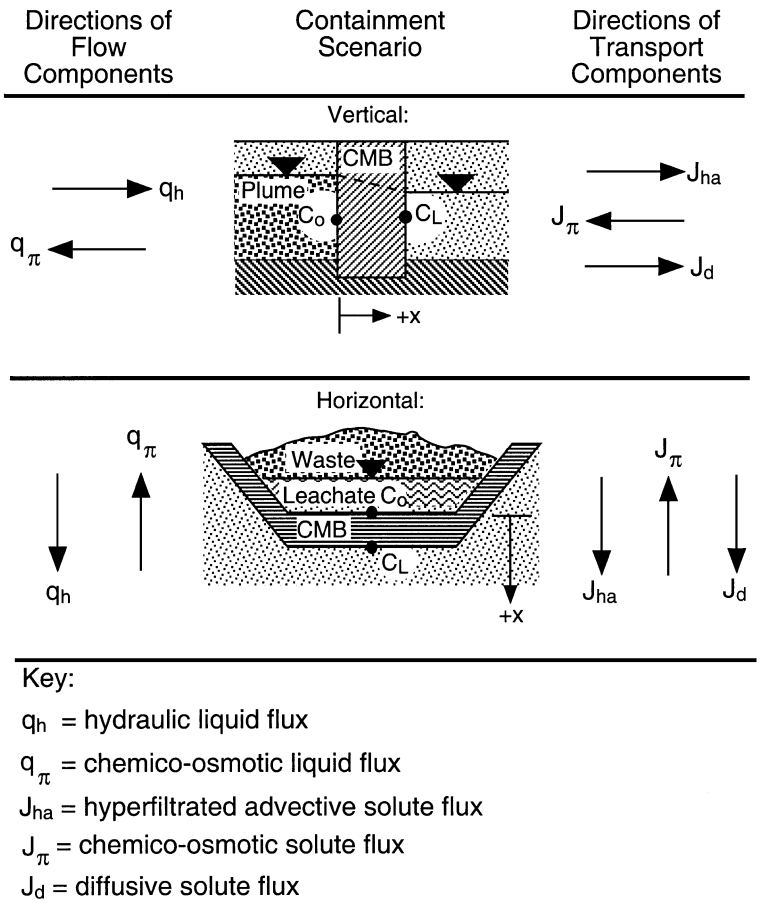

Fig. 4. Vertical and horizontal contaminant scenarios (C_o>C_L) for clay membrane barriers (CMBs) (modified after Shackelford et al., 2001).

of environmental concern. Therefore, determination of the threshold concentrations above which the clay soil no longer exhibits membrane behavior ($\omega = 0$) for a variety of chemical species and testing conditions represents an important practical component in terms of the relevance of membrane behavior for clay soil barriers.

1.5. Clay membrane barriers

As illustrated in Fig. 4, clay barriers that exhibit membrane behavior, or clay membrane barriers (CMBs), can be used in both vertical and horizontal containment scenarios. Vertical containment scenarios typically involve the insertion of a vertical cutoff wall to prevent or minimize the spread of contamination in the subsurface, and usually are employed in applications involving the remediation of contaminated sites (e.g., Shackelford and Jefferis, 2000). Horizontal containment applications typically involve the construction of a liner system used to prevent subsurface contamination in waste disposal applications (e.g., solid waste landfills). However, in both types of applications, the objective of the barrier is to maintain a contaminant concentration at the exit end of the barrier, C_L, lower than the source concentration of the same contaminant, C_o. Thus, by definition, containment implies that $C_L < C_o$.

2. Membrane behavior and chemico-osmotic flow

2.1. General formulation

The total liquid flux through a clay membrane barrier (CMB), q, at steady state includes a hydraulic liquid flux, q_h, in response to the difference in hydraulic head, and a chemico-osmotic liquid flux, q_π, in response to a difference in solute concentration (e.g., Katchalsky and Curran, 1965; Kemper and Rollins, 1966; Olsen et al., 1990), or

$$q = q_h + q_\pi = -k\frac{\Delta h}{L} + \omega\frac{k}{g\rho_w}\frac{\Delta\pi}{L} \quad (1)$$

where k = the hydraulic conductivity of the CMB, Δh (<0) = the head loss across the CMB, L = the thickness of the CMB, g = gravitational acceleration, ρ_w = the mass density of the solution (i.e., essentially the same as water for dilute solutions), and $\Delta\pi$ (<0) = the theoretical chemico-osmotic pressure resulting from the difference in concentration across the barrier.

The theoretical chemico-osmotic pressure difference, $\Delta\pi$, in Eq. (1) can be calculated based on the salt concentrations at the specimen boundaries in accordance with the van't Hoff expression (Katchalsky and Curran, 1965). Although the van't Hoff expression provides only approximate values of the chemico-osmotic pressure difference due to the limiting assumption that the electrolyte solutions are ideal and dilute, Fritz (1986) states that the error associated with the van't Hoff expression is low (<5%) for 1:1 electrolytes (e.g., NaCl, KCl) at concentrations less than 1.0 M. As previously noted, this upper bound in concentration likely is greater than the threshold concentration at which membrane behavior becomes significant for electrolytes.

For a single-salt system, the theoretical chemico-osmotic pressure difference according to the van't Hoff expression is given as follows:

$$\Delta\pi = vRT\Delta C = vRT(C_L - C_o) \quad (2)$$

where v = the number of ions per molecule of the salt, R = the Universal gas constant [8.314 J mol^{-1} K^{-1}], T = the absolute temperature [K], and C = the salt concentration in molarity (M). For example, for KCl solutions ($v = 2$), Eq. (2) becomes:

$$\Delta\pi = 2RT(C_L - C_o) \quad (3)$$

and Eq. (1) becomes:

$$q = q_h + q_\pi = -k\frac{\Delta h}{L} - \omega k\frac{2RT}{g\rho_w}\frac{(C_o - C_L)}{L} \quad (4)$$

As indicated by Eq. (4), the chemico-osmotic liquid flux through the CMB, q_π, occurs from lower solute concentration to higher solute concentration and, therefore, opposes the hydraulic liquid flux, q_h, in typical waste containment applications (see Fig. 4). Thus, if the effect of chemico-osmotic efficiency in the CMB is ignored (i.e., $\omega = 0$), all liquid flux occurs as a hydraulic liquid flux in accordance with Darcy's law (i.e., the first term in Eqs. (1) and (4)).

The relative significance of chemico-osmosis on the total liquid flux through a CMB can be illustrated by considering the ratio, q/q_h, expressed for a simple salt solution (e.g., KCl) as follows:

$$\frac{q}{q_h} = \frac{q}{q_{\omega=0}} = 1 + \omega\frac{2RT}{g\rho_w\Delta h}(C_o - C_L) \quad (5)$$

As indicated by Eq. (5), $q/q_h = 1$ when either $C_o - C_L = 0$ or $\omega = 0$ since no chemico-osmotic liquid flux occurs through the CMB. However, in the case of a horizontal barrier with $\omega > 0$ and $C_o - C_L > 0$, upward chemico-osmotic liquid flux opposes the downward hydraulic liquid flux (i.e., since $\Delta h < 0$). Values of $q/q_h < 0$ indicate that the counter chemico-osmotic liquid flux is sufficiently high such that the net liquid flux is directed into the containment facility, whereas values of $q/q_h > 0$ indicate that the net liquid flux is directed out of the containment facility.

2.2. Simplified analysis for a GCL

The potential significance of membrane behavior on the movement of liquid through a CMB is illustrated herein by considering a geosynthetic clay liner (GCL) containing sodium bentonite as the CMB, as shown schematically in Fig. 5. The depth of ponded liquid is assumed to be 305 mm (1.0 ft), in accordance with the maximum allowable leachate depth for landfills based on current U.S. regulatory standards. Also, the solute concentration in the leachate, C_o, is assumed to be greater than the solute concentration, C_L, at the exit boundary of the GCL, and the GCL is assumed to be saturated by prehydration.

Values of q/q_h versus the difference in KCl concentration across the GCL (i.e., $-\Delta C = C_o - C_L$) for the measured ω values previously shown in Fig. 1b also are shown in Fig. 5. The results based on the measured data indicate that upward liquid flux is likely to occur through the GCL for the range of $-\Delta C$ considered in this study. However, the effect of the membrane behavior eventually will be destroyed and q/q_h will approach unity as values of $-\Delta C$ ($= C_o$) approach the threshold concentrations (see Fig. 2).

A net liquid flux into the containment facility also results in negative advection (i.e., advection in the opposite direction of diffusion) and, thus, is potentially beneficial from the viewpoint of reducing the net rate of contaminant migration out of the containment facility. However, in addition to the limitations resulting from the simplifying assumptions previously noted, the results shown in Fig. 5 neglect the increase in solute concentration with depth due to diffusion and the potential for adverse solute–clay interactions (e.g., see Shackelford et al., 2000). Both of these factors tend to reduce and eventually eliminate the beneficial contribution of chemico-osmotic liquid flux due to compression of the DDLs and a corresponding decrease in ω as the concentration within the GCL increases (Malusis et al., 2001; Malusis and Shackelford, 2002a).

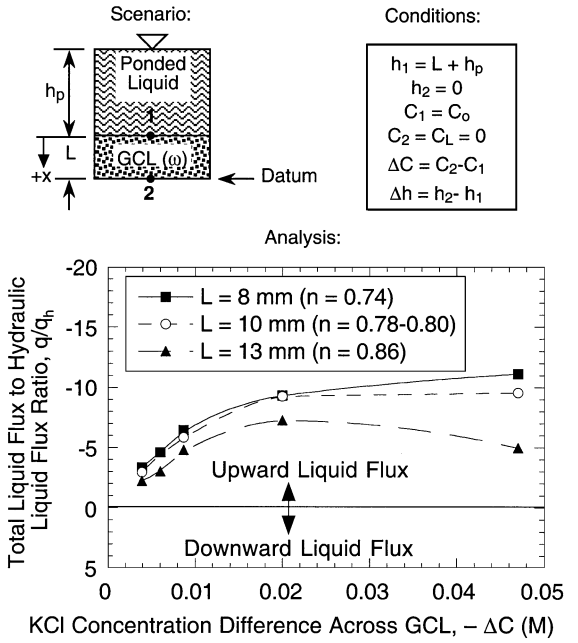

Fig. 5. Results of simplified analysis of the potential effect of membrane behavior on the liquid flux through a GCL (n = porosity, q = total liquid flux, q_h = hydraulic liquid flux).

3. Membrane behavior and solute transport

3.1. General formulation

In the absence of an electrical current, the general expression for total solute (contaminant) flux, J (mass/area/time), in a fine-grained soil (i.e., neglecting

mechanical dispersion) that exhibits membrane behavior can be written for one-dimensional transport as follows (Malusis and Shackelford, 2002b):

$$J = \underbrace{(1-\omega)q_h C}_{J_{ha}} + \underbrace{q_\pi C}_{J_\pi} + \underbrace{nD^* i_c}_{J_d} \quad (6)$$

where D^* = the effective salt-diffusion coefficient as defined by Shackelford and Daniel (1991), i_c = the concentration gradient (>0), and the other parameters are as previously defined. Eq. (6) can be derived for continuous systems from the theory developed by Yeung (1990) and Yeung and Mitchell (1993) by setting the applied current (I) equal to zero in their coupled flux equations and rearranging the resulting expressions (Malusis and Shackelford, 2002b).

For a simple salt (e.g., NaCl), the effective salt-diffusion coefficient in Eq. (6) can be estimated using the Nernst–Einstein equation (Shackelford, 1989), i.e., provided the apparent tortuosity factor is known a priori. However, for more complicated systems involving the simultaneous migration of multiple ionic species, a more elaborate equation based on the approach of Vinograd and McBain (1941) as described by Malusis and Shackelford (2002b) must be used to evaluate the effective salt-diffusion coefficient.

The hyperfiltrated advective solute flux, J_{ha}, in Eq. (6) represents the traditional advective solute flux that is reduced by a factor of $(1-\omega)$ due to the membrane behavior of the soil. In physical terms, the factor $(1-\omega)$ represents the process of hyperfiltration (or ultrafiltration) whereby solutes are filtered out of solution as the solvent passes through the membrane under an applied hydraulic gradient. The second term, J_π, in Eq. (6) is the chemico-osmotic solute flux due to the chemico-osmotic liquid flux, q_π. The third term, J_d, in Eq. (6) represents the diffusive solute flux through soil in the form of Fick's first law as defined by Shackelford and Daniel (1991).

In the limit as $\omega \rightarrow 0$ and, thus, $q_\pi \rightarrow 0$, Eq. (6) reduces to the traditional advective–diffusive solute flux expression. However, as $\omega \rightarrow 1$ (i.e., an "ideal" CMB), the total solute flux given by Eq. (6) should approach zero since, by definition, no solute can enter an ideal or perfect membrane. Thus, the effect of a CMB is to reduce the contaminant (solute) flux through the barrier relative to the contaminant flux that would occur in the absence of membrane behavior. This reduction in the contaminant flux results from two explicit mechanisms: viz., (1) counter advection due to the chemico-osmosis inherent in the J_π term, and (2) solute restriction due to hyperfiltration inherent in J_{ha} term. In addition, the diffusive solute flux must approach zero as ω approaches unity, implying that solute restriction also is inherent in the J_d term. These mechanisms will be discussed in more detail in the following presentation.

3.2. Simplified analysis for a GCL

The potential influence of each of the flux terms shown in Eq. (6) will be discussed within the context of the measured chemico-osmotic efficiency for the GCL specimens corresponding to specimen porosities ranging from 0.78 to 0.80 shown in Fig. 1b, since the thickness of each of these specimens was maintained constant at 10 mm (Malusis and Shackelford, 2002a). In the case of these tests, the source KCl concentration, C_o, was simply twice the average concentration (i.e., $C_o = 2C_{ave}$) since the concentration at the lower boundary of the specimen was maintained essentially at zero. Thus, the measured chemico-osmotic efficiency coefficients, ω, for the GCL can be plotted versus the log of the molar source KCl concentration, as shown in Fig. 6. The results indicate that the threshold source concentration corresponding to incipient membrane behavior, designated

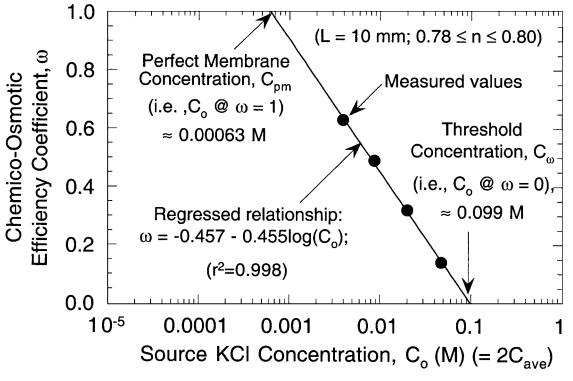

Fig. 6. Measured and regressed chemico-osmotic efficiency coefficients versus source KCL concentration for a 10-mm-thick GCL (data from Malusis and Shackelford, 2002a) (n = specimen porosity).

as C_ω (Shackelford et al., 2001), is approximately 0.099 M KCl based on extrapolation of the fitted function, whereas the source concentration corresponding to perfect membrane behavior, designated as C_{pm} (Shackelford et al., 2001), is $\sim 6.3 \times 10^{-4}$ M KCl.

The lower boundary condition upon which the measured data in Fig. 6 are based commonly is referred to as a "perfectly flushing" boundary condition, and is the same as that assumed in the previous analysis for chemico-osmotic flow (e.g., $C_L = 0$, Fig. 5). From a practical viewpoint, the assumption of a perfectly flushing lower boundary may be appropriate for some field applications, such as scenarios involving vertical cutoff walls, and results in conservative estimates of solute flux for diffusion-dominated transport such as typically occurs through low-permeability ($< 5 \times 10^{-10}$ m/s) clay barriers (Rabideau and Khandelwal, 1998). From a waste containment viewpoint, a perfectly flushing lower boundary may be appropriate, for example, when the GCL serves as the primary or top liner in a double-liner scenario and is underlain by a leachate collection and removal system (LCRS) that removes the leachate at a rate significantly greater than the rate of solute flux through the GCL. Regardless of the possible practical scenario, the validity of the presentation is not lost when the source concentration is used in the analyses because the entire presentation also could be based on an average concentration, as is evident by the equally good semi-log linear fit to the data shown in Fig. 6 relative to the semi-log linear fits to the measured data in Fig. 2.

3.3. Hyperfiltrated solute flux (J_{ha})

The potential influence of membrane behavior in terms of the advective solute flux through the GCL can be illustrated in terms of the fraction of advective flux, f_a, defined as follows:

$$f_a = \frac{J_{ha}}{J_a} = \frac{(1-\omega) q_h C}{q_h C} = 1 - \omega \qquad (7)$$

where J_a = the advective solute flux in the absence of membrane behavior, and all other terms are as previously defined. Based on the measured data and the functional fits to the measured data shown in Fig. 6, the fraction of advective flux for KCl migrating through the 10-mm-thick GCL is shown as a function of the source KCL concentration in Fig. 7a. By definition, the fraction of advective flux must be unity when C_o equals C_ω, and decrease towards zero as C_o approaches C_{pm}.

As previously noted, the same analysis could be performed in terms of the average concentration across a CMB. For example, the trends in f_a versus the average salt concentration across a CMB based on the semi-log linear fits to the measured data shown in Fig. 2 are shown in Fig. 7b. As expected, f_a decreases with decreasing C_{ave} more rapidly for the monovalent salts, and increases with increasing porosity for a given salt and C_{ave}. Thus, the factors that tend to cause a decrease in ω (e.g., increasing

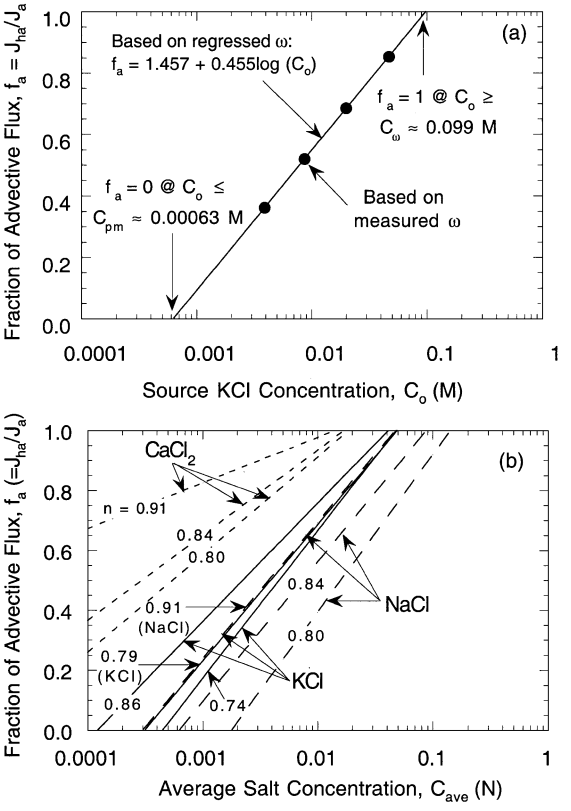

Fig. 7. Fraction of advective solute flux versus salt concentration: (a) results for 10-mm-thick GCL based on measured and fitted data in Fig. 6; (b) results for bentonite specimens based on fitted data in Fig. 2a.

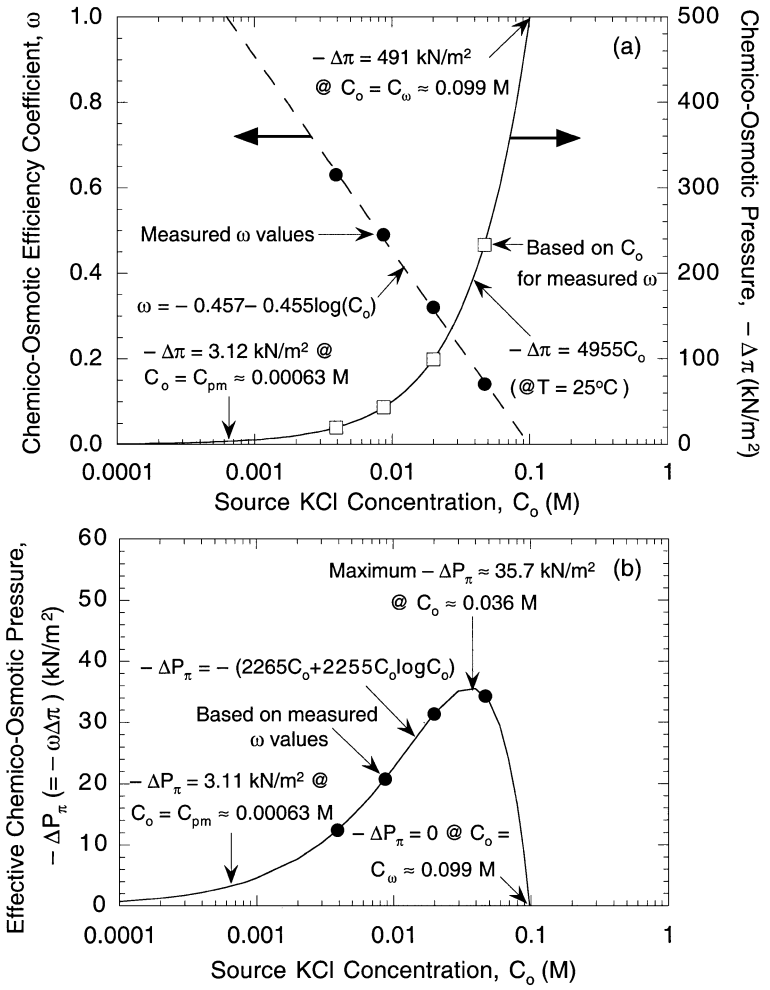

Fig. 8. Effect of source KCl concentration on (a) chemico-osmotic pressure, and (b) effective chemico-osmotic pressure for 10-mm-thick GCL based on measured and fitted data in Fig. 6.

solute concentration, decreasing stress) also cause an increase in f_a, which is consistent with the relationship given by Eq. (7).

3.4. Chemico-osmotic solute flux (J_π)

As noted in Eq. (6), the chemico-osmotic solute flux, J_π, is equal to the product of the chemico-osmotic liquid flux, q_π, and the solute concentration, C, or

$$J_\pi = q_\pi C \tag{8}$$

where, in general, the solute concentration is a function of location and time within the CMB, and q_π, is given by the second term in Eq. (1) as follows:

$$q_\pi = \frac{J_\pi}{C} = \frac{\omega k}{g\rho_w}\frac{\Delta\pi}{L} = \frac{k_\pi}{g\rho_w}\frac{\Delta\pi}{L} \tag{9}$$

where k_π ($=\omega k$) = the chemico-osmotic permeability (Olsen, 1972; Barbour and Fredlund, 1989). Since, $C_L = 0$ in the present case such that $\Delta\pi < 0$ (Eq. (3)), $q_\pi < 0$ and, therefore, $J_\pi < 0$. Thus, the existence of a chemico-osmotic solute flux in this case enhances the containment performance of the GCL. In general, this

enhanced performance will be evident as long as $0 < \omega < 1$. However, if $C_o \geq C_\omega$, then $\omega = 0$ and $J_\pi = 0$ since $q_\pi = 0$. Also, when $C_o \leq C_{pm}$ such that $\omega = 1$, $q_\pi < 0$, but $J_\pi = 0$ because, by definition, complete restriction of the solute (contaminant) results for a perfect membrane such that $C = 0$. Therefore, the magnitude of J_π varies for source concentrations in the range $C_\omega \leq C_o \leq C_{pm}$. This variation in J_π for source concentrations in the range $C_\omega \leq C_o \leq C_{pm}$ results directly from the competing correlations between ω and $\Delta\pi$ versus C_o, since the product of ω and $\Delta\pi$ represents the driving potential for chemico-osmotic counter flux as indicated by the following form of Eq. (9):

$$q_\pi = \frac{J_\pi}{C} = \frac{k}{g\rho_w}\frac{\omega\Delta\pi}{L} = \frac{k}{g\rho_w}\frac{\Delta P_\pi}{L} = k\frac{\Delta h_\pi}{L} = ki_\pi \tag{10}$$

where ΔP_π (<0) = the effective chemico-osmotic pressure, Δh_π (<0) = the effective chemico-osmotic head, and i_π (<0) = the effective chemico-osmotic gradient.

For example, as shown in Fig. 8a, the chemico-osmotic pressure, $-\Delta\pi$, increases with increasing C_o for the GCL scenario currently being considered in accordance with Eq. (3) and $C_L = 0$, whereas ω for the GCL decreases semi-log linearly with increasing C_o, as previously shown in Fig. 6. The result of these two competing trends is a nonlinear variation in ΔP_π such that $-\Delta P_\pi > 0$ (or $\Delta P_\pi < 0$) for all $C_o < C_\omega$, as shown in Fig. 8b.

Two observations are important with respect to the variation in $-\Delta P_\pi$ with C_o shown in Fig. 8b. First, $-\Delta P_\pi$ increases rapidly from zero to a maximum value of approximately 35.7 kN/m^2 as C_o decreases from C_ω ($\approx$ 0.099 M KCl) to approximately 0.036 M KCl, and then $-\Delta P_\pi$ decreases with subsequent decrease in C_o. Thus, the beneficial aspect of increasing solute restriction with increasing ω (e.g., J_{ha}) will be offset to some extent by a decrease in $-\Delta P_\pi$ and, therefore, J_π. Second, $-\Delta P_\pi$ is greater than zero even at $C_o = C_{pm}$ corresponding to $\omega = 1$, so that chemico-osmotic counter flux of liquid will occur through a perfect membrane (i.e., $q_\pi < 0$) even though there can be no chemico-osmotic counter advection (i.e., $J_\pi = 0$) since the concentration of the solute within the GCL must be zero by definition.

Based on Eq. (10), the magnitude of the chemico-osmotic counter flux of liquid, $-q_\pi$ ($= -J_\pi/C$), for the GCL as a function of the source concentration is shown in Fig. 9. The hydraulic conductivity of 1.63×10^{-11} m/s used to generate the curve in Fig. 9 is based on the average of the measured hydraulic conductivities for the four chemico-osmotic tests performed with the GCL (Malusis and Shackelford, 2002a). The trend in $-q_\pi$ versus C_o mimics the trend in $-\Delta P_\pi$ versus C_o as required in accordance with Eq. (10) for a constant hydraulic conductivity and GCL thickness.

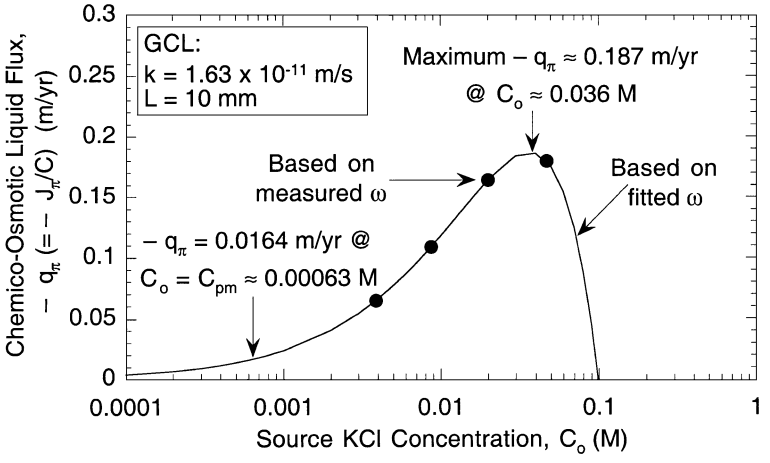

Fig. 9. Effect of source KCl concentration on calculated chemico-osmotic liquid flux for GCL based on measured and fitted data in Fig. 6 (k = hydraulic conductivity; L = GCL thickness).

3.5. Diffusive solute flux (J_d)

The solute restriction inherent in J_{ha} is an "explicit" effect in that $J_{ha} \rightarrow 0$ as $\omega \rightarrow 1$ (Eq. (6)). However, the solute restriction inherent in J_d is not explicitly stated in Eq. (6) and, therefore, is "implicit". This implicit solute restriction results from the correlation between ω and D^* (Malusis and Shackelford, 2002c).

For example, consider the data shown in Fig. 10 based on D^* and ω values from the test results reported by Malusis et al. (2001) for the same GCL for which the data in Fig. 1b were measured. As indicated in Fig. 10, D^* must approach 0 as $\omega \rightarrow 1$ because, by definition, no solute can enter a perfect membrane. At the other extreme, the maximum value of D^*, or $D^*_{(max)}$, will occur when there is no membrane behavior ($\omega = 0$). Thus, D^* for CMBs must decrease from $D^*_{(max)}$ to 0 as ω increases from 0 to 1, respectively, as shown in Fig. 10. As a result, any correct simulation of the contaminant mass flux through a CMB must be based on values of D^* measured at the correct concentration for the application and, therefore, the appropriate ω value. The use of D^* values measured separately from ω at concentrations greater than the "threshold" concentration (i.e., $C_o \geq C_\omega$), e.g., to decrease the testing time, in simulations performed to evaluate contaminant transport through CMBs will neglect this implicit correlation between D^* and ω and, therefore, will be fundamentally incorrect (see Malusis and Shackelford, 2002c).

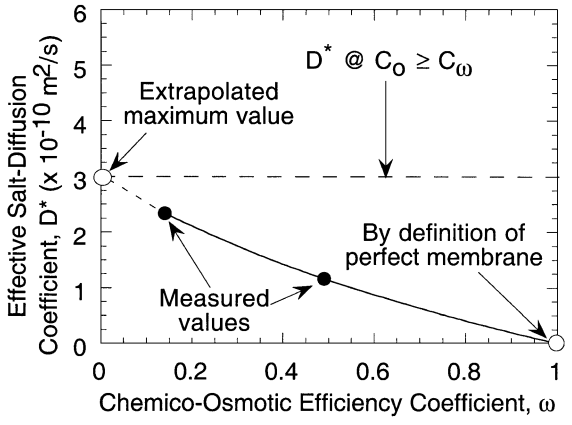

Fig. 10. Effect of chemico-osmotic efficiency on the effective salt-diffusion coefficients for KCl diffusion through a 10-mm-thick GCL at steady state (data from Malusis et al., 2001).

4. Summary and conclusions

After a brief introduction defining membrane behavior, the major factors controlling membrane behavior in clay soils are discussed. In particular, clay soils containing a significant amount of sodium montmorillonite, such as sodium bentonite, have been shown to exhibit membrane behavior. Since such clay soils also are typically used as containment barriers (e.g., soil–bentonite cutoff walls, geosynthetic clay liners, compacted sand–bentonite liners) for geoenvironmental applications, the existence of membrane behavior may have an effect on the migration of solutes through such clay soil barriers.

The flux equations for flow and transport through clay membrane barriers (CMBs) used in waste containment and remediation applications are presented and discussed. The results of a simplified analysis of flow through a geosynthetic clay liner (GCL) using measured values for the chemico-osmotic efficiency coefficient (ω) of the GCL indicate that membrane behavior can result in a total liquid flux that actually counters the outward Darcy liquid flux due to chemico-osmotic counter flow.

Also, the effect of a CMB is shown to reduce the contaminant mass flux through the barrier relative to the contaminant mass flux that would occur in the absence of membrane behavior due to two mechanisms: counter advection due to chemico-osmosis, and contaminant (solute) restriction. Contaminant restriction results explicitly from hyperfiltration and implicitly from the correlation between the chemico-osmotic efficiency coefficient, ω, and the effective diffusion coefficient, D^*, of the contaminant.

Acknowledgements

This paper represents an extension of a recently completed joint research effort between Colorado State University (CSU) and the Colorado School of Mines (CSM), funded by the U.S. National Science Foundation (NSF), Arlington, VA, under Grant CMS-9616854 for CSU and Grant CMS-9616855 for CSM.

The opinions expressed in this paper are solely those of the writers and are not necessarily consistent with the policies or opinions of the NSF.

References

Abichou, T., Benson, C.H., Edil, T.B., 2002. Foundry green sands as hydraulic barriers: field study. Journal of Geotechnical and Geoenvironmental Engineering, ASCE 128 (3), 206–215.

Barbour, S.L., Fredlund, D.G., 1989. Mechanisms of osmotic flow and volume change in clay soils. Canadian Geotechnical Journal 26, 551–562.

Chapuis, R.P., Lavoie, J., Girard, D., 1992. Design, construction, performance, and repair of the soil–bentonite liners of two lagoons. Canadian Geotechnical Journal 29 (4), 638–649.

D'Appolonia, D.J., 1980. Soil–bentonite slurry trench cutoffs. Journal of the Geotechnical Engineering Division, ASCE 106 (4), 399–417.

Day, S.R., 1994. The compatibility of slurry cutoff wall materials with contaminated groundwater. In: Daniel, D.E., Trautwein, S.J. (Eds.), Hydraulic Conductivity and Waste Contaminant Transport in Soil, ASTM STP 1142. ASTM, West Conshohocken, PA, pp. 284–299.

Fritz, S.J., 1986. Ideality of clay membranes in osmotic processes: a review. Clays and Clay Minerals 34 (2), 214–223.

Garlanger, J.E., Cheung, F.K., Bishar, S.T., 1987. Quality control testing for a sand–bentonite liner. In: Woods, R.D. (Ed.), Geotechnical Practice for Waste Disposal '87. ASCE, Reston, VA, pp. 488–499.

Gipson Jr., A.H., 1985. Permeability testing on clayey soil and silty sand–bentonite mixture using acid liquor. In: Johnson, A.I., et al. (Eds.), Hydraulic Barriers in Soil and Rock, ASTM STP 874. ASTM, West Conshohocken, PA, pp. 140–154.

Gleason, M.H., Daniel, D.E., Eykholt, G.R., 1997. Calcium and sodium bentonite for hydraulic containment applications. Journal of Geotechnical and Geoenvironmental Engineering, ASCE 123 (5), 438–445.

Grathwohl, P., 1998. Diffusion in Natural Porous Media, Contaminant Transport, Sorption/Desorption and Dissolution Kinetics. Kluwer Academic Publishing, Norwell, MA, USA.

Greenberg, J.A., Mitchell, J.K., Witherspoon, P.A., 1973. Coupled salt and water flows in a groundwater basin. Journal of Geophysical Research 78 (27), 6341–6353.

Hanshaw, B.B., Coplen, T.B., 1973. Ultrafiltration by a compacted clay membrane: II. Sodium ion exclusion at various ionic strengths. Geochimica et Cosmochimica Acta 37 (10), 2311–2327.

Katchalsky, A., Curran, P.F., 1965. Nonequilibrium Thermodynamics in Biophysics. Harvard Univ. Press, Cambridge, MA, USA.

Keijzer, Th.J.S., Kleingeld, P.J., Loch, J.P.G., 1997. Chemical osmosis in compacted clayey material and the prediction of water transport. In: Yong, R.N., Thomas, H.R. (Eds.), Geoenvironmental Engineering, Contaminated Ground: Fate of Pollutants and Remediation. Thomas Telford Publ., London, pp. 199–204.

Kemper, W.D., Rollins, J.B., 1966. Osmotic efficiency coefficients across compacted clays. Soil Science Society of America, Proceedings 30, 529–534.

Jo, H.Y., Katsumi, T., Benson, C.H., Edil, T.B., 2001. Hydraulic conductivity and swelling on nonprehydrated GCLs permeated with single-species salt solutions. Journal of Geotechnical and Geoenvironmental Engineering, ASCE 127 (7), 557–567.

Lundgren, T.A., 1981. Some bentonite sealants in soil mixed blankets. Proceedings, 10th International Conference on Soil Mechanics and Foundation Engineering, Stockholm, Sweden, June 15–19, vol. 2. A.A. Balkema, Rotterdam, The Netherlands, pp. 349–354.

Malusis, M.A., Shackelford, C.D., 2002a. Chemico-osmotic efficiency of a geosynthetic clay liner. Journal of Geotechnical and Geoenvironmental Engineering, ASCE 128 (2), 97–106.

Malusis, M.A., Shackelford, C.D., 2002b. Theory for reactive solute transport through clay membrane barriers. Journal of Contaminant Hydrology, vol. 59 (3–4). Elsevier, Amsterdam, pp. 291–316.

Malusis, M.A., Shackelford, C.D., 2002c. Coupling effects during steady-state solute diffusion through a semipermeable clay membrane. Environmental Science and Technology, ACS 36 (6), 1312–1319.

Malusis, M.A., Shackelford, C.D., Olsen, H.W., 2001. A laboratory apparatus to measure chemico-osmotic efficiency coefficients for clay soils. Geotechnical Testing Journal, ASTM 24 (3), 229–242.

Mitchell, J.K., 1993. Fundamentals of Soil Behavior, 2nd ed. Wiley, New York, USA.

Olsen, H.W., 1969. Simultaneous fluxes of liquid and charge in saturated kaolinite. Soil Science Society of America, Proceedings 33, 338–344.

Olsen, H.W., 1972. Liquid movement through kaolinite under hydraulic, electric, and osmotic gradients. American Association of Petroleum Geologists Bulletin 56 (10), 2022–2028.

Olsen, H.W., Yearsley, E.N., Nelson, K.R., 1990. Chemico-osmosis versus diffusion–osmosis. Transportation Research Record, vol. 1288. Transportation Research Board, Washington, DC, pp. 15–22.

O'Sadnick, D.L., Simpson, B.E., Kasel, G.K., 1995. Evaluation and performance of a sand/bentonite liner. In: Acar, Y.B., Daniel, D.E. (Eds.), Geoenvironment 2000. ASCE, Reston, VA, pp. 688–701.

Rabideau, A., Khandelwal, A., 1998. Boundary conditions for modeling transport in vertical barriers. Journal of Environmental Engineering, ASCE 124 (11), 1135–1140.

Ryan, C.R., 1987. Vertical barriers in soil for pollution containment. In: Woods, R.D. (Ed.), Geotechnical Practice for Waste Disposal '87. ASCE, Reston, VA, pp. 182–204.

Shackelford, C.D., 1989. Diffusion of contaminants through waste containment barriers. Transportation Research Record, vol. 1219. Transportation Research Board, Washington, DC, pp. 57–64.

Shackelford, C.D., Daniel, D.E., 1991. Diffusion in saturated soil: I. Background. Journal of Geotechnical Engineering, ASCE 117 (3), 467–484.

Shackelford, C.D., Jefferis, S.A., 2000. Geoenvironmental engineering for in situ remediation. International Conference on

Geotechnical and Geoenvironmental Engineering (GeoEng2000), Melbourne, Australia, Nov. 19–24, vol. 1. Technomic Publ., Lancaster, PA, USA, pp. 126–185.

Shackelford, C.D., Benson, C.H., Katsumi, T., Edil, T.B., Lin, L., 2000. Evaluating the hydraulic conductivity of GCLs permeated with non-standard liquids. Geotextiles and Geomembranes 18 (2–4), 133–161.

Shackelford, C.D., Malusis, M.A., Olsen, H.W., 2001. Clay membrane barriers for waste containment. Geotechnical News, vol. 19 (2). BiTech Publ., Richmond, BC, Canada, pp. 39–43.

Staverman, A.J., 1952. Non-equilibrium thermodynamics of membrane processes. Transactions of the Faraday Society 48, 176–185.

Stern, R.T., Shackelford, C.D., 1998. Permeation of sand-processed clay mixtures with calcium chloride solutions. Journal of Geotechnical and Geoenvironmental Engineering, ASCE 124 (3), 231–241.

Vinograd, J.R., McBain, J.W., 1941. Diffusion of electrolytes and of the ions in their mixtures. Journal of the American Chemical Society 63, 2008–2015.

Yeung, A.T., 1990. Coupled flow equations for water, electricity and ionic contaminants through clayey soils under hydraulic, electrical, and chemical gradients. Journal of Non-Equilibrium Thermodynamics 15, 247–267.

Yeung, A.T., Mitchell, J.K., 1993. Coupled fluid, electrical, and chemical flows in soil. Geotechnique 43 (1), 121–134.